Available online at www.sciencedirect.com
ScienceDirect
Thermochimica Acta 458 (2007) 138–147
thermochimica acta
www.elsevier.com/locate/tca

The influence of the tryptophan point mutation on the stability of tetracycline repressor (TetR)

Sylwia Kędracka-Krok *, Zygmunt Wasylewski ✠

Department of Physical Biochemistry, Faculty of Biochemistry, Biophysics and Biotechnology, Jagiellonian University, Krakow, Poland

Available online 12 January 2007

Abstract

The influence of a point mutation on the thermal stability of the tetracycline repressor (TetR) was studied with differential scanning calorimetry (DSC) and circular dichroism (CD) measurements, performed at pH 8.0. Single tryptophan TetR mutants, namely TetR W43 and TetR W75, were chosen because they had been used as fluorescence probes in structural investigations of TetR. The DSC results show that in the absence of tetracycline, the thermally induced transitions of all proteins can be described as irreversible process, strongly dependent upon scan rate. The observed scan dependence indicates that the protein denaturation is under kinetic control described by simple kinetic scheme: $N_2 \xrightarrow{k} F_2$, where k is first-order kinetic constant, N_2 the native state and F_2 is the final, denatured state. The replacement of tryptophan by phenylalanine at position 43 located on the solvent accessible surface of TetR WT (mutant TetR W75) results in a slight increase in the denaturation temperature (T_{max}), whereas Trp75Phe substitution located in the core of TetR WT (mutant TetR W43) induces a strong decrease of T_{max}. These opposing effects are discussed in the frame of structural changes of modified proteins. The effect of tetracycline (Tc) binding on the DSC transitions of TetR tryptophan mutants is also shown. Based on the observed increase of the T_{max}, it is concluded that the binding of Tc to the mutants causes strong enhancement of their stability. Moreover, in case of TetR W43 the Tc binding compensates the stability loss due to introduced mutation.

Keywords: Tet repressor; Tetracycline; Differential scanning calorimetry (DSC); Circular dichroism (CD); Thermal denaturation

1. Introduction

The tetracycline repressor (TetR) controls the production of the membrane protein (TetA) which makes Gram-negative bacteria resistant to the antibiotic, tetracycline. In brief, TetR acts as a molecular switch for this resistance. In the absence of tetracycline (Tc) in the bacterial cell, the TetR binds to specific operator sites preventing the biosynthesis of TetA. The penetration of Tc into the cell leads to formation of the $[MgTc]^+$ complex which binds to the TetR and reduces its affinity to DNA. As a consequence, synthesized TetA conducts active Tc efflux via the $[MgTc]^+/H^+$ antiporter embedded in the plasma membrane.

Each monomer of homodimeric TetR consists of 207 residues folded into 10 α helices. The helices α1–α3 at the N-end of polypeptide chain constitute the small, N-terminal domain responsible for interaction with DNA. The seven remaining α helices create a regulatory C-terminal domain having a tunnel-like inducer ($[MgTc]^+$) binding pocket. The TetR protein and its mutants together with the *tet* operator create a very efficient inducible system of gene expression in higher eukaryotes [1,2]. Chemically induced denaturation of the wild type of TetR (TetR WT) has been described in literature as a two-state reversible process [3]. Recently, the thermally induced denaturation of TetR WT has been characterized by the simplest two-state irreversible denaturation model [4].

Tryptophan residues of the single tryptophan mutants called TetR W43 (contains Trp only at position 43) and TetR W75 (possesses Trp only at position 75) were very often used in the past as convenient fluorescent probes in studies of properties of TetR tertiary structure, its dynamics and the kinetics of TetR interaction with Tc and DNA [5–10]. Both residues are highly conserved and occur in all classes of tetracycline repressor proteins [11]. They are located in regions which are important for protein function. Trp W43 is exposed to the solvent surface of

Abbreviations: TetR, tetracycline repressor; TetR W43, single tryptophan mutant with Trp only at position 43; TetR W75, single tryptophan mutant with Trp only at position 75; WT, wild type; DSC, differential scanning calorimetry; DLS, dynamic light scattering; CD, circular dichroism

* Corresponding author. Fax: +48 12 66 46 902.
E-mail address: sylwia@mol.uj.edu.pl (S. Kędracka-Krok).

✠ This paper is dedicated to my mentor, Zygmunt Wasylewski, who died during the preparation of it on 27 July 2006.

0040-6031/$ – see front matter © 2007 Elsevier B.V. All rights reserved.
doi:10.1016/j.tca.2007.01.001

the DNA-binding domain, precisely in the helix α3, belonging to the helix-turn-helix (HTH) motive, whereas Trp 75 is located in the neighborhood of hydrophobic, Tc-binding pocket, i.e. at helix α5, which is involved in the formation of the protein core.

The characterization of modified proteins is usually limited to the description of the differences in their secondary structure based on comparative circular dichroism (CD) measurements. In the case of the Trp mutants the analysis of far UV (190–250 nm) CD spectra does not reveal any significant differences in the contents of their secondary structures in comparison to TetR WT [12]. However, it is generally agreed that the most common and easy CD test is an insufficient verification of possible changes in the structure of the mutated protein. Moreover, it should be obligatory to quantify the changes in protein stability caused by an introduced mutation.

The aim of the present studies was to investigate the influence of Trp → Phe substitution on the TetR stability by thermal denaturation using differential scanning calorimetry (DSC) and circular dichroism (CD) methods. Dynamic light scattering (DLS) technique was applied in addition.

2. Experimental

2.1. Materials

2.1.1. N.B. – addresses required – town and country of suppliers

Acrylamide, phenylmethylsulfonyl fluoride (PMSF), tetracycline and Tris were purchased from Sigma. Dithiotreitol (DTT), magnesium chloride hexohydrate and sodium chloride were from Fluka. The Fractogel EMD SO^{3-} 650 (M) was from Merck, while the Q Sepharose Fast Flow and Sephacryl S-200 HR were from Amsterdam Pharmacia Biotech. The nutrients for bacterial growth were from Life Technologies . All other chemicals were products of analytical-grade from POCh-Gliwice. Buffers in water purified by the Millipore system were used throughout this work.

2.2. Protein purification

The single tryptophan mutants TetR W43 and TetR W75 were overproduced in *Escherichia coli*, strain RB 791, containing the appropriate plasmid, pWH1950.

Protein purification in general followed the scheme described by Ettner et al. [13] with a few modifications [9]. After the purification procedure, the protein was highly pure (>97%) as judged by SDS-polyacrylamide gel electrophoresis and Coommasie Brilliant Blue staining. The concentration of dimer TetR variants was determined spectrophotometrically using the following excitation coefficients: $\varepsilon_{280\,nm} = 22 \times 10^3\ M^{-1}\ cm^{-1}$ [6] and $20.7 \times 10^3\ M^{-1}\ cm^{-1}$ (estimated from amino acid sequence [14]) for TetR W43 and TetR W75, respectively. The activity of the proteins was checked using the tetracycline titration method. The concentration of tetracycline was determined in 0.1 M HCl using the excitation coefficient of $\varepsilon_{355\,nm} = 13{,}320\ M^{-1}\ cm^{-1}$ [8].

All measurements for unliganded proteins were performed in buffer A: 10 mM Tris, 150 mM NaCl, 2 mM DTT, pH 8.0, but for the complexes of TetR variants with tetracycline, buffer B was used, which additionally contained 10 mM $MgCl_2$. A comparison of the calorimetric enthalpy and the denaturation temperature for the studied proteins in the absence of Tc, in buffer with and without Mg ions, did not show any differences in these values. The Tris buffer exhibits a pronounced dp/dT dependence. However the results were not significantly affected by pH change with increasing temperature. The presented data were obtained in the same buffer condition and they have a mainly comparative character.

2.3. Differential scanning calorimetry (DSC)

These experiments were performed on a CSC 6100 Nano II Differential Scannnig Calorimeter (Lindon, UT (USA)) with a vessel volume of 0.3228 ml, interfaced with an IBM-compatible PC. The concentrations of the protein samples were in the range of 0.4–4.0 mg/ml and there were different scanning-rates of 0.1–2.0 K/min. Before the measurements, the protein samples were intensively dialyzed against buffer A, and the samples with tetracycline against buffer B. The samples and reference solutions were degassed for at least 5 min at room temperature and carefully loaded into the vessels to avoid bubble formation. The vessels were cleaned carefully before each experiment. A constant pressure of 304 kPa was always maintained to prevent possible degassing of the samples upon heating. A background scan recorded with the buffer in both cells was subtracted from each test scan. The reversibility of thermal transitions was checked by examining the reproducibility of calorimetric trace in the second heating of sample immediately after fast cooling from the first scan.

The excess molar heat capacity (C_p^{exc}) was calculated using the molecular weight of TetR variants of 46,708 Da and partial specific volume of protein of 0.73 ml/g [15]. The Origin software package (Microcal, Northampton, MA (USA)) was used for baseline subtraction and determination of total enthalpy change. Integration of the transition curves was done numerically. Molar transition enthalpies ΔH referring to the molecular weight of the protein and the van't Hoff enthalpies (ΔH_{vH}) were calculated according to the van't Hoff equation:

$$\Delta H_{vH} = \frac{A R T_{max}^2 C_p^{exc,max}}{\Delta H_{cal}}, \quad (1)$$

where $C_p^{exc,max}$ is the excess of molar specific heat capacity over the base line value at maximum of transition, T_{max} is the denaturation temperature in degrees kelvin (K), ΔH_{cal} is the total molar enthalpy change during denaturation process, R the gas constant and A is equal to 4.0 for monomer or for the nondissociated dimer [16].

2.4. Circular dichroism (CD)

CD measurements were performed on a Jasco-710 spectropolarimeter (Tokyo, Japan) equipped with a water-jacketed cell holder and a Julabo F25 (Seelbach, Germany) circulator bath

with programmable temperature controller. The actual temperature inside the quartz cell (with path length of 1 mm) was measured with a Digi-sence thermocouple thermometer (Cole-Parmer Instrument Company, Vernon Hills, Illinois (USA)). Protein thermal denaturation was monitored by the changes in ellipticity at 222 nm with scanning-rate of 1 K/min. Spectra were collected in temperature range between 25 and 85 °C. Analysis of the data and determination of midpoint melting temperature (T_m) values were performed by noise reduction and differentiation of curves using the Standard Analysis program provided with the instrument.

2.5. Dynamic light scattering (DLS)

These measurements were made using a DynaPro-MS800 instrument from Protein Solution Inc. (Charlottesville, VA). All samples were filtered through a 0.02 μm membrane (Whatman, Anodisc 13) into a 45 μl (3 mm path length) quartz cuvette. The measurements were performed at 20 ± 0.1 °C. DLS data were analyzed by autocorrelation method to calculate the translational diffusion coefficient (D_T) of the TetR mutants and their complexes with tetracycline. The results were analyzed by using monomodal and bimodal models. The hydrodynamic radius (R_H) is derived from D_T using the Stokes–Einstein equation:

$$R_H = \frac{k_B T}{6\pi\eta D_T} \quad (2)$$

where k_B is the Boltzman constant, T temperature in Kelvin and η is the solvent viscosity. The theoretical hydrodynamic radius (R_H^{theo}) can be obtained from: $R_H^{theo} = [(3M(v+h))/(4\pi N_A)]^{1/3}$, where N_A is the Avogadro constant, v the partial specific volume, h the hydration, and M is the molar mass of the protein. The ratio R_H/R_H^{theo} provides information about the shape of the molecule in the solution.

3. Results

3.1. DSC measurements

Both the TetR Trp variants and their complexes with tetracycline underwent irreversible denaturation under all adopted conditions, even if the sample was cooled immediately after the peak absorption was completed and then it was scanned again, or when the heating was stopped near maximum point and then the sample was cooled and reheated. An aggregation was evident in the samples extracted from calorimetric vessel. Additionally, an exothermic peak was present for higher protein concentrations on the high-temperature side of the DSC endotherm.

3.2. The concentration effect

The thermograms for the TetR muteins were measured in buffer A as a function of protein concentration from 0.4 to 4.0 mg/ml at scanning-rate of 1.0 K/min. The typical

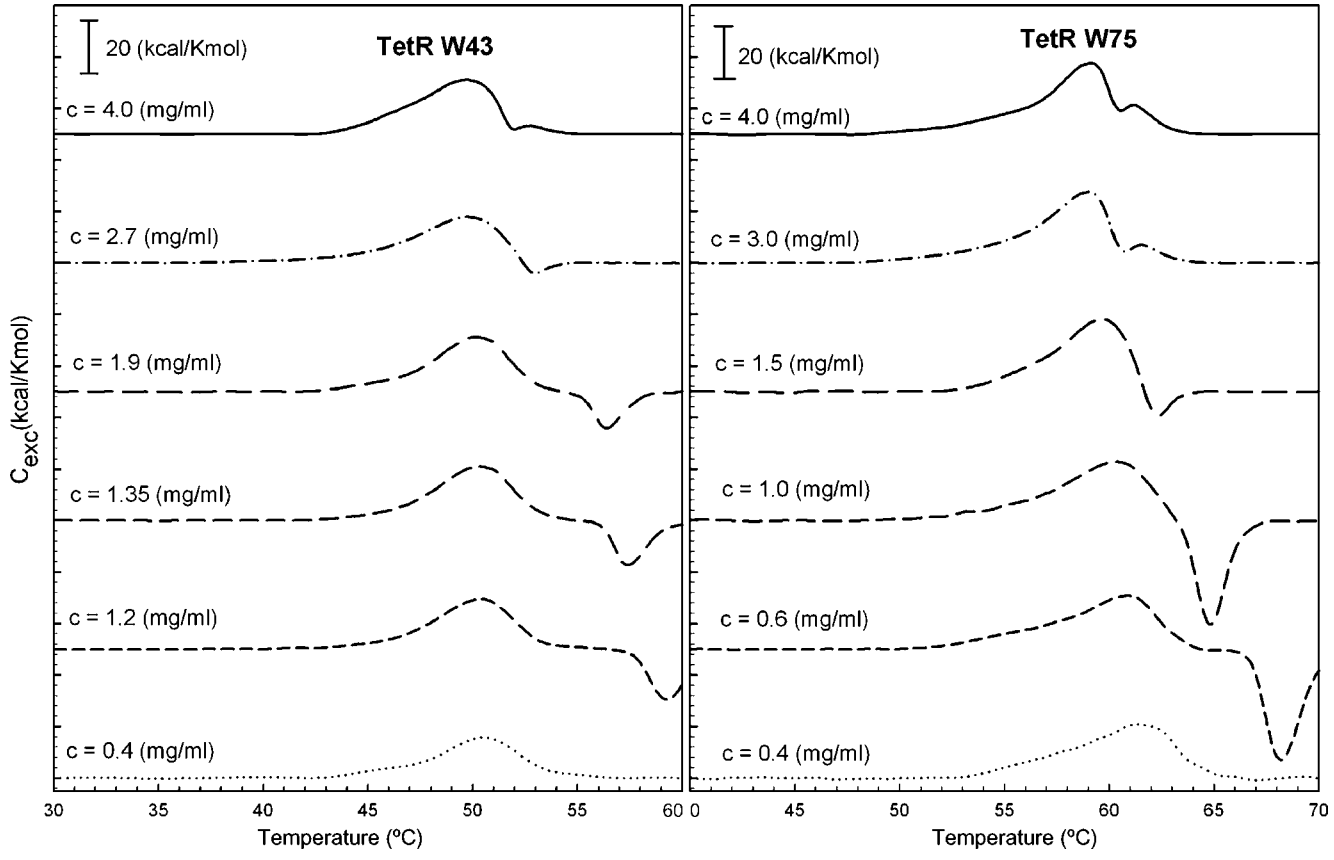

Fig. 1. Typical thermograms for single tryptophan mutants of TetR at different protein concentrations. Measurements were made in buffer A: 10 mM Tris buffer pH 8.0 with 150 mM NaCl and 2 mM DTT, at a scanning-rate of 1 K/min.

Table 1
Apparent thermodynamic transition parameters for TetR W43 and TetR W75 at various protein concentrations

TetR W43[a]				TetR W75[a]			
c (mg/ml)	T (°C)	ΔH_{cal} (kJ/mol)	$\Delta H_{cal}/\Delta H_{vH}$	c (mg/ml)	T (°C)	ΔH_{cal} (kJ/mol)	$\Delta H_{cal}/\Delta H_{vH}$
0.32[b]	50.39			0.40[b]	60.66		
0.41	50.4	293.84	0.36	0.40	61.3	511.14	0.80
0.75	49.6	410.70	0.59	0.50	61.3	514.20	0.72
1.19	50.4	402.28	0.57	0.60	60.9	505.61	0.79
1.35	50.3	420.84	0.58	1.00	60.3	527.23	0.78
1.88	50.1	416.61	0.56	2.00	59.7	511.05	0.60
2.70	49.7	397.30	0.61	3.00	59.0	516.92	0.63
4.00	50.0	399.52	0.58	4.00	59.1	488.26	0.56
Average standard deviation	50.03 ± 0.32	391.60 ± 44.00	0.55 ± 0.08		60.23 ± 0.98	510.64 ± 11.94	0.70 ± 0.10

[a] Buffer: 10 mM Tris, 150 mM NaCl, 2 mM DTT, pH 8.0.
[b] Parameters obtained from CD measurements.

denaturation curves for both Trp mutants at different protein concentrations are presented in Fig. 1. The values of T_{max} at different concentrations of the protein are given in Table 1. The obtained T_{max} decrease with the increasing protein concentrations for both mutants but for TetW43 only very slightly.

As for wild type of tetracycline repressor [4], the enthalpic effect accompanying the aggregation process of TetR variants is pronounced above the concentration of 0.4 mg/ml, and cannot be neglected. Furthermore, in the DSC thermograms for the TetR mutants, the minimum of the negative peak shifts towards the lower temperature and the exotherm intensity decreases with increasing protein concentration. From Fig. 1, it is evident that the protein concentration influences both endothermic and exothermic parts of the DSC curve in the same direction, viz. both peaks shift towards the low-temperature side with increasing concentration. However, this effect is greater for the exothermic peak than for the endothermic one. As a consequence, at a high protein concentration (about 4.0 mg/ml) the two peaks almost overlap.

The obtained DSC profiles for TetR mutants are highly asymmetric and the ratio $\Delta H_{cal}/\Delta H_{vH}$ is much below unity, i.e. at about 0.55 and 0.70 for TetR W43 and for TetR W75, respectively (see Table 1). This indicates a tendency of the TetR mutants to form aggregates. As can be judged from the dependence of T_{max} values on protein concentration, the oligomerization level for TetR W43 seems to be independent of the protein concentration over the range used in these studies but for TetR W75 the oligomerization slightly increases with increasing concentration of protein. The measured calorimetric enthalpy change, ΔH_{cal}, although determined with some inaccuracy because of the existence of the exothermic peak, is independent of concentration for both proteins (Table 1).

3.3. The effect of the scanning-rate

The thermal denaturation of the TetR proteins was carried out at the protein concentration of 0.6 mg/ml and the scanning-rate ranging between (v) 0.1–2.0 K/min. The calorimetric enthalpy values of the denaturation process as a function of the scan rate are shown in Table 2. For both proteins, TetR W43 and TetR W75, the measured T_{max} exhibits an increasing linear dependence on the scanning-rate as seen in Fig. 2. These results indicate that the denaturation of TetR variants occurs as a kinetically controlled process, which cannot be described by equilibrium thermodynamics [17–21]. It was assumed out that the observed phenomenon can be described on the basis of a simplest two-state irreversible model:

$$N_2 \xrightarrow{k} F_2, \quad \text{(I)}$$

in which only the native (N_2) and the final (F_2) states are significantly populated and the transformation from N_2 to F_2 is strongly temperature-dependent. This kind of the denaturation process is

Table 2
Apparent thermodynamic transition parameters of TetR W43 and TetR W75 at various heating rates

TetR W43[a]			TetR W75[a]		
v (K/min)	ΔH_{cal} (kJ/mol)	$\Delta H_{cal}/\Delta H_{vH}$	v (K/min)	ΔH_{cal} (kJ/mol)	$\Delta H_{cal}/\Delta H_{vH}$
0.2	369.98	0.54	0.5	494.84	0.76
0.7	392.10	0.64	1.0	371.99	0.54
1.0	413.51	0.58	1.2	582.91	1.10
1.2	433.20	0.65	1.5	490.65	0.77
1.5	455.58	0.72	1.8	486.79	0.77
1.8	462.24	0.70	2.0	526.60	0.78
2.0	443.39	0.67			
Average standard deviation	424.28 ± 34.06	0.64 ± 0.06		492.28 ± 69.14	0.78 ± 0.18

[a] Buffer: 10 mM Tris, 150 mM NaCl, 2 mM DTT, pH 8.0.

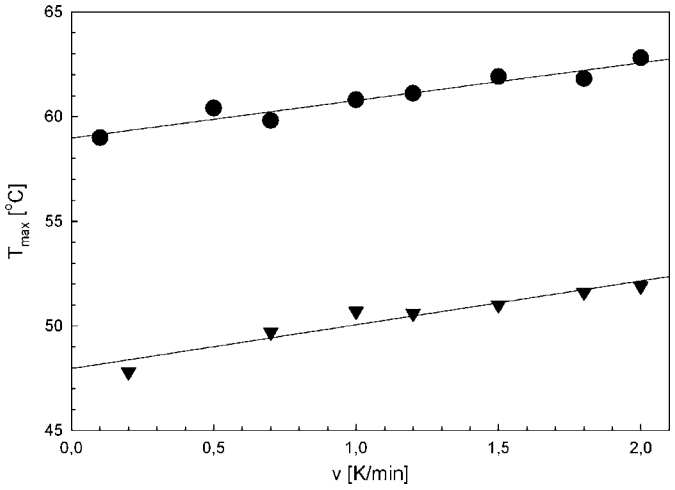

Fig. 2. Effect of scanning-rate on transition temperature. Data obtained from DSC experiments. The circles (●) correspond to T_{max} for TetR W75, the triangles (▼) correspond to T_{max} for TetR W43. The continuous lines have no theoretical meaning and are shown to guide the eye.

assumed to be the first-order reaction with the rate constant, k, that changes with temperature, according to the Arrhenius equation:

$$k = A \exp\left(-\frac{E_a}{RT}\right) = \exp\left\{\left(\frac{E_a}{R}\right)\left(\frac{1}{T^*} - \frac{1}{T}\right)\right\}$$

where E_a is the activation energy and T^* is the temperature at which $k = 1\,\text{min}^{-1}$ (the frequency factor is equal to $\exp(E/RT^*)$).

To check the validity of the two-state kinetic model for description of presented denaturation data, the activation energy, E_a, was calculated using the approach proposed by Sanchez-Ruiz [17,22] according to following equations:

$$k = \frac{v\Delta C_p^{exc}}{\Delta H - Q}, \tag{3}$$

$$\ln\left\{\ln\left[\frac{Q}{\Delta H - Q}\right]\right\} = \frac{E_a}{R((1/T_m) - (1/T))}, \tag{4}$$

$$\frac{v}{T_m^2} = \left(\frac{AR}{E_a}\right)\exp\left(-\frac{E_a}{RT_m}\right), \tag{5}$$

$$E_a = \frac{eRT_m^2\Delta C_p^{exc,max}}{\Delta H}, \tag{6}$$

where v (K/min) corresponds to the scan rate, ΔH the total heat of the process, Q the heat evolved up to a given temperature corresponding to the total area below the thermogram between the initial and given temperatures T, ΔC_p^{exc} the excess heat capacity, T_m the temperature at maximum of heat capacity curve, R the gas constant, $\Delta C_p^{exc,max}$ the heat capacity at trace maximum, and e is the base of the natural logarithm. The experimental results of the Arrhenius plots described by these equations are presented in Fig. 3 and the calculated values of the activation energy are shown in Table 3. As can be seen in Table 3, the obtained kinetic parameters exhibit a good coincidence, which supports the idea that the thermal transitions of TetR proteins are well described

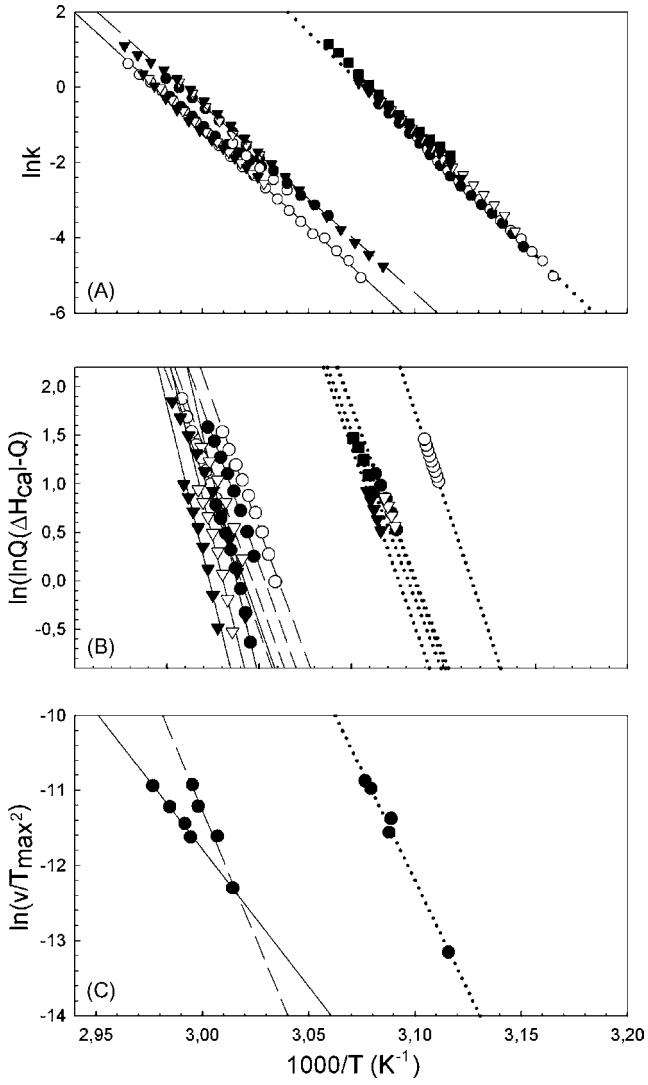

Fig. 3. (A) Arrhenius plot including the rate constant (k) values corresponding to different scanning-rates ((◯) −0.2 °C/min, (●) −1.0 °C/min, (▽) −1.2 °C/min, (▼) −1.8 °C/min, (■) −2.0 °C/min for TetR W43) ((◯) −1.0 °C/min, (●) −1.2 °C/min, (▽) −1.5 °C/min, (▼) −2.0 °C/min for TetR W75) ((◯) −0.5 °C/min, (●) −1.0 °C/min, (▽) −1.5 °C/min, (▼) −2.0 °C/min for TetR WT). The reaction rate constants at given temperature T were obtained by using Eq. (3). A plot of ln k vs. $1/T$ gives straight line (dotted, broken and solid for TetR W43, TetR W75 and TetR WT, respectively). (B) The plots according Eq. (4). give linear dependence with slope $-E_A/R$. The symbols are the same as those used in (A). (C) Straight lines represents the plots according Eq. (5). The symbols are the same as those used in (A). The protein concentration was in all cases 0.6 mg/ml.

by the two-state kinetic model. The excess heat capacity curves of both mutants acquired at different scan rates are presented in Fig. 4. The experimental data were fitted according to the equation described by Conejero-Lara et al. [23]:

$$C_p^{exc} = eC_p^{exc,max}\exp\left[\frac{E_a(T - T_m)}{RT_m^2}\right] \times \exp\left[\exp\left[\frac{E_a(T - T_m)}{RT_m^2}\right]\right]. \tag{7}$$

Table 3
Arrhenius equation parameters estimated from the two-state irreversible model of thermal denaturation of TeR WT, TetR W43 and TetR W75 according to Eqs. (3)–(7)

v (K/min)	E_a (kJ/mol)				
	Eq. (3)	Eq. (4)	Eq. (5)	Eq. (7)	Eq. (6)
TetR WT[a]					
0.50	407.70	421.84	411.74	367.50	
1.00	410.80	429.10	430.58	427.69	
1.50	437.99	430.01	433.55	415.69	
2.00	419.28	423.42	436.64	431.67	
Average	418.94 ± 13.61	426.09 ± 4.07	428.13 ± 11.20	410.64 ± 29.55	420.06 ± 22.11
TetR W43[a]					
0.2	457.77	471.50	468.17	455.28	
0.7	419.27	428.57	416.74	410.68	
1.0	459.09	429.16	487.63	472.07	
1.2	440.6	427.39	450.41	437.42	
1.5	402.37	460.31	430.86	423.06	
1.8	422.13	440.16	447.93	433.86	
2.0	438.31	422.79	447.85	433.03	
Average	434.22 ± 20.8	439.98 ± 18.7	449.94 ± 23.2	437.91 ± 20.3	439.15 ± 20.01
TetR W75[a]					
0.50	406.07	453.15	444.75	424.40	
1.00	429.33	452.34	466.55	453.52	
1.20	365.07	452.16	361.17	354.85	
1.50	432.62	436.41	434.39	437.87	
1.80	416.69	468.95	431.02	427.09	
2.00	418.72	438.97	460.09	447.19	
Average	411.42 ± 24.61	450.33 ± 11.71	432.99 ± 37.85	424.15 ± 35.76	428.30 ± 27.14

[a] Buffer: 10 mM Tris, 150 mM NaCl, 2 mM DTT, pH 8.0.

Theoretical traces, according to Eq. (7) reflect well the obtained experimental data. The calculated values of the activation energy are scanning-rate independent (see Table 3) which additionally confirms the use of the kinetic two-state model. The mean values of E_a are 440 ± 20 and 429 ± 27 kJ/mol for TetR W43 and TetR W75, respectively.

3.4. The influence of tetracycline presence on the DSC profiles of TetR proteins

Illustrative thermograms for TetR mutants and their complexes with tetracycline measured at 0.4 mg/ml protein concentration and 1 K/min heating rate are shown in Fig. 5. As can be seen, the ligand binding causes an enhancement of the symmetry of the curves and a significant increase of the denaturation temperature. The obtained T_{max} values are equal to 50.4 °C and 61.3 °C for TetR W43 and TetR W75, respectively. The denaturation temperatures, T_{max}, of the complexes of TetR variants with tetracycline are equal to 71.4 and 73.5 °C for TetR W43 and TetR W75. Therefore, under the present experimental conditions, the binding of tetracycline causes an increase of the T_{max} of the protein of about 21.0 and 12.2 °C for TetR W43 and for TetR W75, respectively, while this difference for TetR WT under the same conditions was of about 10.0 °C [4]. The ligand binding results in the two fold increase of the denaturation enthalpy in case of both mutants (see the legend of Fig. 5).

3.5. CD measurements

The CD measurements were performed in the same buffer conditions as the DSC experiments. Fig. 6 shows a representative CD denaturation profile for the TetR variants. The shape of the first derivative of the CD profiles is similar to the DSC thermograms. The obtained CD results confirm the tendency in the behavior of the transition temperature observed with DSC method (Table 1). Converted to the mean residue ellipticity, the CD thermal transition spectra for both proteins were analyzed using nonlinear least square fitting and the results are presented in Fig. 6. The fraction of denatured protein F_U was calculated from the spectral parameter used to follow the denaturation (y) prior to the minimization procedure according to the relationship: $F_U = (y - y_N)/(y_U - y_N)$; $y_N = a_1 + a_2T$ and $y_U = b_1 + b_2T$ are the means of y characteristic of the native and denatured conformation, respectively. They were obtained by linear regression of pre- and post-transitional baseline. The parameter used to observe the denaturation y, can be expressed as a function of the kinetic parameters according to the following equation [24]:

$$y = y_U - [y_U - y_N] \exp\left\{-\frac{1}{v}\int_{T_0}^{T} \exp\left[\frac{E_a}{R}\left(\frac{1}{T^*} - \frac{1}{T}\right)\right] dT\right\}. \quad (8)$$

The kinetic parameters obtained from the analysis of CD curves are: 372.13 ± 1.33 and 396.16 ± 2.24 kJ/mol for E_a and

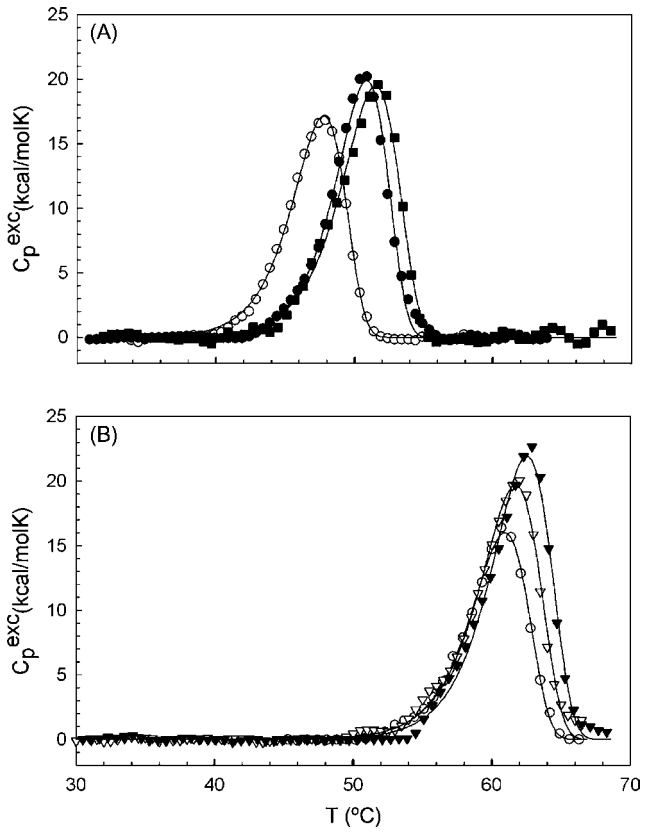

Fig. 4. Temperature dependence of the excess molar heat capacity of TetR W43 and TetR W75 at different scan rate. In panel (A) thermograms for TetR W43 at heating rate of 0.2 K/min (◯), 1.0 K/min (●), 2.0 K/min (■). In panel (B) thermograms for TetR W75 at heating rate of 1.0 K/min (◯), 1.5 K/min (▽), 2.0 K/min (▼). Solid lines are the best fits to each curve according to Eq. (7). The protein concentration was always 0.6 mg/ml. Measurements were performed in buffer A: 10 mM Tris buffer pH 8.0 with 150 mM NaCl and 2 mM DTT.

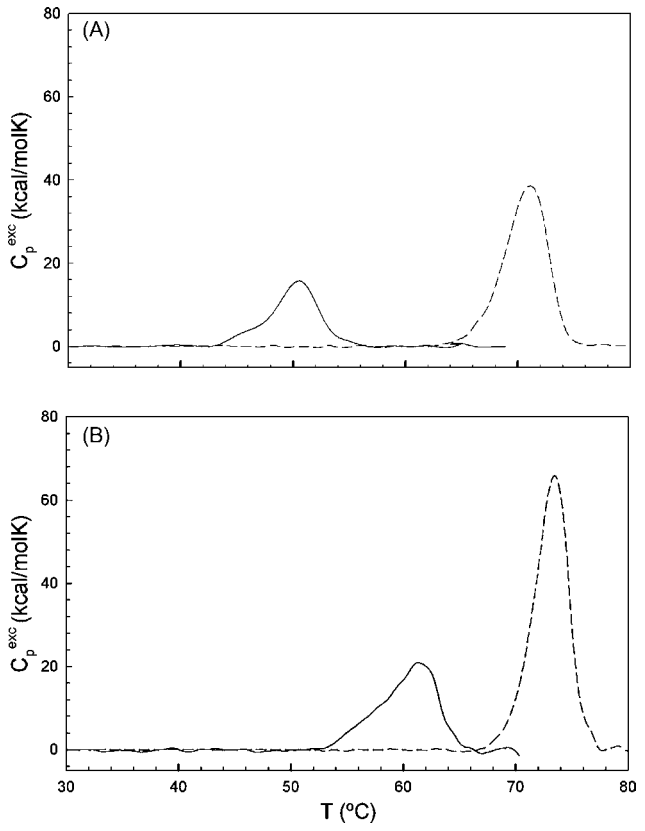

Fig. 5. Typical thermograms of TetR (solid line) and complex of TetR with tetracycline (broken line) for TetR W43 and TetR W75 in panels (A) and (B), respectively. Obtained ΔH_{cal} 801 and 1059 kJ/mol for TetR W43-[Tc-Mg]$^+$ and TetR W75-[Tc-Mg]$^+$, respectively. Measurements were made in buffer A: 10 mM Tris buffer pH 8.0 with 150 mM NaCl and 2 mM DTT, at a scanning-rate of 1 K/min and buffer B: 10 mM Tris buffer pH 8.0 with 150 mM NaCl, 2 mM DTT and 10 mM $MgCl_2$, at a scanning-rate of 1 K/min, for TetR alone and for the complex of TetR with tetracycline, respectively. The concentration of the protein in all cases was 0.4 mg/ml. The ratio of concentrations was 5 mol Tc per 1 mol of TetR dimer.

51.84 ± 0.02 and 63.33 ± 0.03 °C for T^* for TetR W43 and TetR W75, respectively.

3.6. DLS measurements

In the DLS experiments, the buffer conditions were the same as in the DSC measurements. The curves showing the estimated hydrodynamic radius of TetR variants as a function of protein concentration are presented in Fig. 7. In order to evaluate the R_H^{theo} value, it was assumed that the hydration was 0.2 g H_2O/g protein and the partial specific volume was 0.73 cm^3/g protein [15,25]. The hydrodynamic radii R_H values (obtained from linear extrapolation to zero concentration) is of 3.03 ± 0.02 and 2.96 ± 0.03 nm for TetR W43 and TetR W75, respectively. A R_H/R_H^{theo} ratio higher than 1 (about 1.15) reveals similar discrepancies in the spherical shape of the proteins. The increasing linear dependence of the R_H on the concentration of TetR mutants, up to about 1 mg/ml, suggests a strong tendency of the protein to aggregation. In higher concentrations, the R_H seems to be almost constant. Therefore it can be suggested that under these conditions the protein molecules themselves exert a stabilizing effect.

4. Discussion

Similarly to the wild type TetR^B [4], its single tryptophan mutants TetR W43 and TetR W75 examined with DSC and CD methods undergo the irreversible denaturation upon increasing temperature. Because the mutants under study are homodimeric proteins, it was necessary to check whether or not there is dissociation. The changes in the oligomerization state of the protein during the denaturation process should be revealing in the concentration dependence of T_{max}. The observed, admittedly slight, decrease of T_{max} for TetR W75 and TetR W43 as a function of the protein concentration indicates the existence of an aggregation process which often is accompanied by the kinetic-controlled thermally-induced denaturation. At higher protein concentrations, the irreversibility is associated with exothermic phenomena, frequently observed for aggregating systems [21]. The obtained ratios of $\Delta H_{cal}/\Delta H_{vH}$ for both mutant proteins are much below the unity that also indicates the presence of the aggregation process. However, this parameter can be treated only qualitatively in the case of irreversible transitions. The results of the DLS measurements conducted at

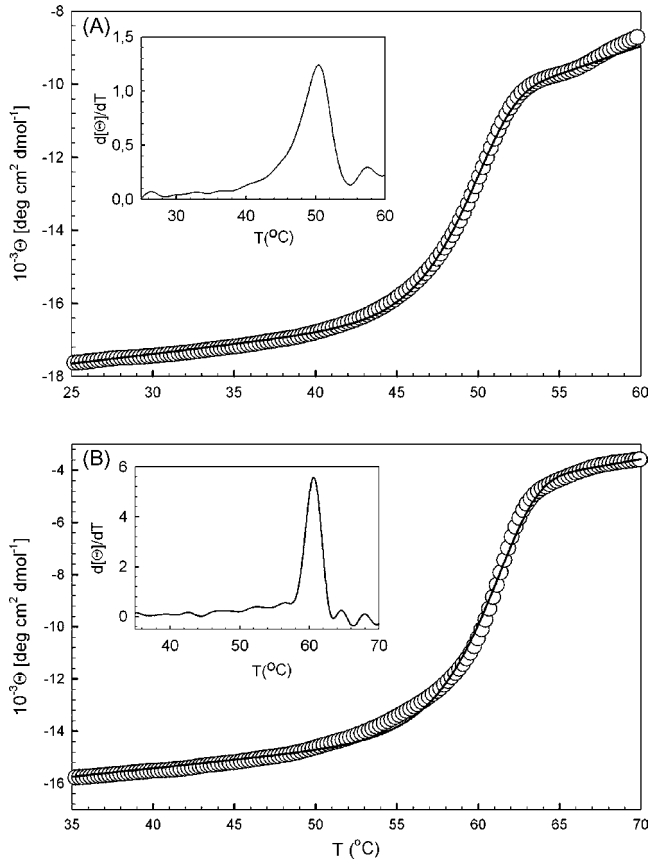

Fig. 6. Temperature-dependence of residue ellipticity at 222 nm for TetR W43 (panel A) and TetR W75 (panel B) in buffer A (10 mM Tris buffer pH 8.0 with 150 mM NaCl and 2 mM DTT) obtained on heating with constant scan rate of ≈1 K/min. The solid line is the best fit obtained using Eq. (8). Inset: temperature derivative ellipticity vs. temperature.

20 °C also support the suggestion that the main reason for the irreversibility of unfolding process is the protein aggregation.

The DSC transition curves are strongly scanning-rate dependent and are highly asymmetric, particularly at the lower heating rate. This means that the state of the protein in solution depends on the time necessary to reach a given temperature. Thus, the thermal denaturation of TetR mutants is under kinetic control and the shape of the DSC curves is distorted by irreversible alterations in a consecutive step of the denaturation process, as described by the Lumry-Eyring model [17]. Analysis of the DSC transitions was performed on the basis of a limiting Lumry-Eyring model assuming the simplest two-state irreversible denaturation process (I). The estimated averages of the Arrhenius equation parameters obtained from Eqs. (3)–(7) are in a good agreement with each other, which strongly supports the use of the examined model to explain the TetR protein denaturation. The fitting of the CD denaturation curves according to Eq. (8) also confirms the correctness of the chosen two-state irreversible model. The evaluated averaged values of E_a is of 440 ± 20 and 429 ± 27 kJ/mol for TetR W43 and TetR W75, respectively; and they are close to each other and also to the value of 420 ± 16 (and 414 ± 15 from [4]) calculated for TetR WT. The values of E_a for the Tet variants are comparable with those obtained for other proteins of similar size (for example -553 ± 21 kJ/mol for 5-enoylopyruvate shikimat-3-phosphate synthetase [26], −345–376 kJ/mol for lectin [27] or -300 ± 20 and 342 ± 12 kJ/mol for procarboxypeptidase A and B [28,23]). However, the values for the calorimetric enthalpy, ΔH_{cal}, equal to 408 ± 39, 501 ± 35 and 495 ± 76 kJ/mol for TetR W43, TetR W75 and TetR WT (Tables 1 and 2 from [4]), respectively, are significantly lower than those values detected for all above mentioned proteins. Nevertheless, some other bacterial regulatory, homodimeric proteins of similar size, have almost identical values for ΔH_{cal}, for example −504 kJ/mol for CRP (cAMP receptor protein) [29] or −505 kJ/mol for MetR (methionine repressor protein) [30]. It should be noted that among the Tet proteins used in the present study, TetR W43 has relatively the highest E_a in comparison to its ΔH_{cal}, which suggests the presence of high level of unfolded protein population before the irreversible step of denaturation.

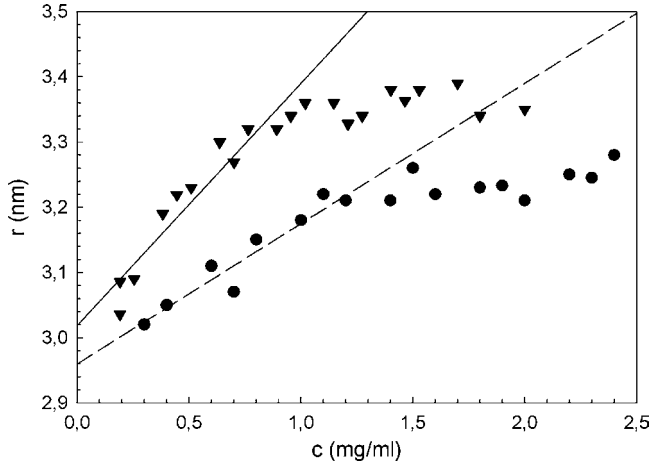

Fig. 7. Dependence of hydrodynamic radii on concentration of TetR W43 (▼) and TetR W75 (●) in buffer A.

The most pronounced distinction between the TetR mutants is the difference in the value of T_{max} of about 11 °C. In the case of irreversible denaturation, the $T_{max,}$ defined as the lowest temperature at which significant denaturation (loss of the native state) occurs in the relevant timescale, is a useful gauge to describe the operational protein stability. In this context, under the whole investigated range of the concentration and scanning-rates, the TetR W43 appears to be much less stable (−10 °C) and TetR W75 slightly more stable (+1 °C) than the wild type TetR.

The substitution Trp43Phe in TetR W75 can be classified as a surface mutation, located at the solvent-exposed area of the protein, whereas Trp75Phe substitution in TetR W43 is an internal mutation in the buried, hydrophobic region of TetR [31]. Generally, the surface point mutation does not trigger any repacking of the protein core. This type of modification also does not induce any significant changes in the solvent accessibility of the native and denaturated states of the mutant in comparison to corresponding native and denaturated states of the wild type protein. As a consequence, the mutation at position 43 exerts only a small effect on the TetR stability. The observed inconsiderable increase of T_{max} for TetR W75 with respect to TetR WT can result of small differences in the propensity of the Trp and Phe residues to form the α helix formation. The helix propensity,

thought as an intrinsic preference of an amino acid to be in the helical conformation, is a result of an energetically optimal arrangement of dihedral angles but also depends on a local environment of a given amino acid in a particular protein [32]. The hydrophobic Phe residue is more favorable in α helix structure than polar side chain of Trp amino acid and in this way promotes the TetR W75 stability.

The observed dramatic decrease of the stability of TetR W43 requires careful consideration. Tryptophan 75 is the second residue at the N-terminal of the α helix 5, which together with four helix bundles (α8, α8′, α10, α10′) forms the rigid core of the TetR. The mutation maintains the aromatic character of the amino acid but the spatial properties of the Trp and Phe rings are different. Thus, the substitution of the double, hetero-cyclical indol ring of the Trp for the smaller benzene ring of the Phe leads to the creation of a cavity in the well-packed TetR interior and a lowering in the protein stability. As is known from literature, cavity-creation mutations like the substitution Leu → Ala in, for example, 4-α-helix- bundle of ROP protein (repressor of *primer*) [33,34], likewise the exchange Trp → Phe (for example in the apomyglobin [35]) significantly destabilize the native state of the protein. The transition enthalpy change (ΔH_{cal}) for TetR W43 (408 ± 39 kJ/mol) is noticeably lower than that for TetR WT (495 ± 76 kJ/mol), which indicates the unfavorable energetic changes associated with the point mutation at position 75.

On the other hand, the Trp 75 is located in the nearest neighborhood of Ser 74, the first residue at the N-terminal α-helix 5. Ser 74, together with Asp77, is involved in the formation of a helix capping box at the N-terminus of α5 of TetR. The helix capping box is defined by the pattern following: N-cap-X-X-3N. At the position of N-cap, the following residues can be found: Ser, Thr and more seldom Asn, Asp, Gln, Glu and Cys and at the position 3N: Gln and Asp, however, the pair: Ser/Thr at N-cap and Glu at the 3N exhibits the strongest preference. The substitution Trp75Phe can indirectly influence the strength of a hydrogen bond between the Ser74 and Asp77 (if it does not make it impossible at all) and in consequence, destabilizes the α-helix 5.

There is no clear evidence providing a uniform mechanism for the observed stability changes upon exchange of Trp to Phe in position 75. Two mentioned mechanisms, namely the cavity creation and the disturbance of the capping box of the helix α5, may contribute to the apparent decrease in stability. However, a quantitative explanation of the experimental data obtained for the mutants is difficult because their effects propagate beyond the site of mutation, through the sequence and three-dimensional structure, known as a compensation nature of the protein.

The preliminary data concerning the influences of ligand binding on mutant stability are sufficiently informative to draw some interesting conclusions. The tetracycline binding significantly increases the protein stability of both mutants. Moreover, in the case of TetR W43, it almost completely compensates for the stability loss due to the mutation (Fig. 7). Furthermore, the mutations do not perturb the proteins function as can be judged from previous kinetic measurements [10]. There are two pieces of kinetic evidence that mutations do not change the function of the single Trp mutants. Firstly, the models describing the kinetics of the ligand binding are the same for Trp mutants and for TetR WT. Secondly, the first step of the association process is characterized by very similar values of kinetic constants and binding constants K_{ass} for all of the proteins. From the earlier, mainly crystallographic studies it is known that Tc interacts, among others, with the residues Asn 82 and Phe 86 which are located in the helix α5 [36]. Thus, the preservation of the induction function and the rebuilding of TetR W43 mutant stability results from the reconstruction of the appropriate connections between the amino acids in the protein molecule or/and creating the new connections between the amino acids by the tetracycline entering into protein binding pocket thereby minimizing of the disturbances of the protein structure. The local binding of the Tc to the TetR W43 leads to a global increase of the protein stability manifested by a very significant increase of the denaturation temperature. The results presented here concerning the influence of the Tc on the TetR W43 stability are the new evidence that small, nonpolar ligand accommodated within or near the mutant internal cavity restores the protein stability. The compensation effects due to the propagation of the destabilizing influence of mutation and the expansion of stabilizing influence of the ligand binding are also the reasons why all consequences of the mutation are unlikely to be predicted from a computer modeling. Thus, the effects of each protein mutation on the stability and function of protein should be empirically determined by DSC and other biophysical methods.

Acknowledgements

We thank Professor W. Hillen for supplying the *E. coli* strain overproducing TetR proteins. The author acknowledges Prof. Marta Dziedzicka-Wasylewska and Ewelina Fic for careful reading of the manuscript.

References

[1] W. Saenger, P. Orth, C. Kisker, W. Hillen, (NO '%') Hinrichs, Angew. Chem. Int. Ed. 39 (2000) 2042–2052.
[2] P. Orth, D. Schnappinger, W. Hillen, W. Saenger, W. Hinrichs, Nat. Struct. Biol. 7 (2000) 215–219.
[3] W. Backes, Ch. Berens, V. Helbl, S. Walter, F.X. Schmid, W. Hillen, Biochemistry 6 (1997) 5311–5322.
[4] S. Kędracka-Krok, Z. Wasylewski, Eur. J. Biochem. 270 (2003) 4564–4573.
[5] P.S. Antonioni, W. Hillen, N. Ettner, W. Hinrich, P. Fantucci, S.M. Doglia, J.-A. Bousquet, M. Chabbert, Biophys. J. 72 (1997) 1800–1811.
[6] C. Peviani, W. Hillen, N. Ettner, H. Lami, S.M. Doglia, E. Piémont, C. Ellouze, M. Chabbert, Biochemistry 34 (1995) 13007–13015.
[7] M. Chabbert, W. Hillen, D. Hansen, M. Takahashi, J.-A. Bousquet, Biochemistry 31 (1992) 1951–1960.
[8] M. Takahashi, L. Altschmied, W. Hillen, J. Mol. Biol. 187 (1986) 341–348.
[9] S. Kędracka-Krok, Z. Wasylewski, J. Protein Chem. 18 (1999) 117–125.
[10] S. Kędracka-Krok, A. Górecki, P. Bonarek, Z. Wasylewski, Biochemistry 44 (2005) 1037–1046.
[11] W. Hillen, Ch. Berens, Annu. Rev. Microbiol. 48 (1994) 345–369.
[12] P. Kaszycki, A. Guz, M. Drwięga, Z. Wasylewski, J. Protein Chem. 15 (1996) 607–619.
[13] N. Ettner, G. Müller, Ch. Berens, H. Backes, D. Schnappinger, T. Schreppel, K. Pfleiderer, W. Hillen, J. Chromatogr. A 742 (1996) 95–105.
[14] S.C. Gill, P. von Hippel, Anal. Biochem. 182 (1989) 319–326.

[15] S.J. Perkins, Eur. J. Biochem. 157 (1986) 169–180.
[16] J.M. Sturtevant, Ann. Rev. Phys. Chem. 38 (1987) 463–488.
[17] J.M. Sanchez-Ruiz, Biophys. J. 61 (1992) 921–935.
[18] E. Freire, W.W. van Osodol, O.L. Mayorga, J.M. Sanchez-Ruiz, Ann. Rev. Biophys. Biophys. Chem. 19 (1990) 159–188.
[19] J.M. Sanchez-Ruiz, Subcel. Biochem. 24 (1995) 133–176.
[20] J.R. Lepock, K.P. Ritchie, M.C. Kolios, A.M. Rodahl, K.A. Heinz, J. Kruuv, Biochemistry 31 (1992) 12706–12712.
[21] I.M. Plaza del Pino, B. Ibarra-Molero, J.M. Sanchez-Ruiz, Proteins Struct. Funct. Genet. 40 (2000) 58–70.
[22] J.M. Sanchez-Ruiz, J.L. Lopez-Locomba, M. Cortijo, P.L. Mateo, Biochemistry 27 (1988) 1648–1652.
[23] F. Conejero-Lara, P.L. Mateo, F.X. Aviles, J.M. Sanchez-Ruiz, Biochemistry 30 (1991) 2067–2072.
[24] B.I. Kurganov, A.E. Lyubarev, J.M. Sanchez-Ruiz, V.L. Shnyrov, Biophys. Chem. 69 (1997) 125–135.
[25] C.R. Cantor, P.R. Schimmel, Biophysical Chemistry, W.H. Freedman & Company, New York, USA, 1980.
[26] E.K. Marabet, M.C. Walker, H.K. Yuen, J.A. Sikorski, Biochim. Biophys. Acta 1161 (1993) 272–278.
[27] M.J. Marcos, R. Chehin, J.L. Arrondo, G.G. Zhadan, E. Villar, V.L. Shnyrov, FEBS Lett. 443 (1999) 192.
[28] J.M. Sanchez-Ruiz, J.L. Lopez-Locomba, P.L. Mateo, M. Vilanova, M.A. Serra, F.X. Aviles, Eur. J. Biochem. 176 (1988) 225–230.
[29] U. Błaszczyk, Z. Wasylewski, J. Protein Chem. 22 (2003) 285–293.
[30] C.M. Johnson, A. Cooper, P.G. Stockley, Biochemistry 31 (1992) 9717–9724.
[31] E. Freire, Methods Mol. Biol. 168 (2001) 37–68.
[32] J.K. Myers, N.C. Pace, M. Scholtz, Biochemistry 36 (1997) 10923–10929.
[33] C. Steif, H.-J. Hinz, G. Cesareni, Proteins 23 (1995) 83–96.
[34] A.M. Buckle, P. Cramer, A.R. Fersht, Biochemistry 35 (1996) 4298–4305.
[35] M.S. Kay, R.L. Baldwin, Nat. Struct. Biol. 3 (1996) 439–445.
[36] P. Orth, F. Cordes, D. Schnappinger, W. Hillen, W. Saenger, W. Hinrchs, J. Mol. Biol. 279 (1998) 439–447.